Acidovorax pan-genome reveals specific functional traits for plant beneficial and pathogenic plant-associations

Roberto Siani[1,2], Georg Stabl[3], Caroline Gutjahr[3], Michael Schloter[1,2], Viviane Radl[1*]

[1] Helmholtz Center for Environmental Health, Institute for Comparative Microbiome Analysis; Ingolstaedter Landstr. 1; 85758 Oberschleissheim, Germany

[2] Technical University of Munich, School of Life Sciences, Chair for Soil Science; Emil-Ramann-Strasse 2; 85354 Freising, Germany

[3] Technical University of Munich, School of Life Sciences, Plant Genetics; Emil-Ramann-Strasse 4; 85354 Freising, Germany

*Corresponding author:

viviane.radl@helmholtz-muenchen.de

phone +49 89 3187 2903

Keywords:

Acidovorax, plant growth promotion, plant pathogens, *Lotus japonicus*, comparative genome analysis

Abstract

Beta-proteobacteria belonging to the genus *Acidovorax* have been described from various environments. Many strains can interact with a range of hosts, including humans and plants, forming neutral, beneficial or detrimental associations. In the frame of this study we investigated genomic properties of 52 bacterial strains of the genus *Acidovorax*, isolated from healthy roots of *Lotus japonicus,* with the intent of identifying traits important for effective plant-growth promotion. Based on single-strain inoculation bioassays with *L. japonicus*, performed in a gnotobiotic system, we could distinguish 7 robust plant-growth promoting strains from strains with no significant effects on plant-growth. We could show that the genomes of the two groups differed prominently in protein families linked to sensing and transport of organic acids, production of phytohormones, as well as resistance and production of compounds with antimicrobial properties. In a second step, we compared the genomes of the tested isolates with those of plant pathogens and free-living strains of the genus *Acidovorax* sourced from public repositories. Our pan-genomics comparison revealed features correlated with commensal and pathogenic lifestyle. We could show that commensals and pathogens differ mostly in their ability to use plant-derived lipids and in the type of secretion-systems being present. Most free-living *Acidovorax* strains did not harbour any secretion-systems. Overall, our data indicated that *Acidovorax* strains undergo extensive adaptations to their particular lifestyle by horizontal uptake of novel genetic information and loss of unnecessary genes.

38 **Introduction**

39 Several soil-derived bacteria, which can colonize plant roots, directly or indirectly promote
40 plants' health by facilitating nutrient mobilization and uptake [1], altering plant hormone levels
41 hormones [2] and competing with pathogens [3, 4]. At the same time, soils also harbour a large
42 repertoire of plant pathogens. It is not entirely clear what distinguishes non-harmful root-
43 associated commensals from pathogens, as even closely related strains have been proven to
44 promote plant-growth or, contrariwise, to negatively affect it [5]. Several studies [6, 7] link this to
45 loss or acquisition of genomic features [e.g., virulence factor, pathogenicity islands], resulting
46 from mutations and horizontal gene transfer [8]. Our existing knowledge in this field is still
47 scarce and inconsistent, as in most cases only single strains were compared, which does not
48 allow to understand evolutionary patterns and to define a generalized model.

49 Bacteria of the genus *Acidovorax* belong to the group of Gram-negative beta-proteobacteria [9]
50 and form associations with a wide range of monocotyledonous and dicotyledonous plants [10].
51 *Acidovorax* has been mostly considered as biotrophic pathogen [11]. However, bacteria of this
52 genus are also known as commensal species or plant beneficial bacteria, which produce
53 secondary metabolites and hormones promoting plant growth, as well as competing with
54 pathogens [12]. Most common species are *A. delafieldii* and *A. facilis*, whilst the most studied
55 pathogenic species is *A. avenae*, the agent of corn (*Zea mays)*, sugar cane (*Saccharum*
56 *officinarum)* and rice (*Oryza sativa)* leaf blight, orchids brown spot disease and watermelon
57 (*Citrullus lanatus)* fruit blotch. Thus, *Acidovorax* is a valuable model organism to investigate
58 evolutionary patterns of plant-associated bacteria and to study which genes differentiate
59 bacteria acting as biotrophic pathogens, as commensals or plant growth-promoting bacteria
60 [13].

61 In the frame of this study, we compared the genomes of isolates classified as *Acidovorax* which
62 were obtained from roots of healthy *Lotus japonicus* ecotype Gifu plants. We tested the strains
63 for their ability to promote plant growth of *L. japonicus* in sterilized sand and correlated
64 differences in the genomes of the strains to the observed effects on plant growth. For a broader
65 comparative analysis, we included additional genomes, available in public databases, belonging

66 to strains from 15 different species of *Acidovorax* from different environments, including all
67 major groups of plant pathogens from this genus. We studied the diversity in the pan-genome
68 and critically evaluated enriched gene functions, secondary metabolites biosynthetic clusters in
69 the different functional groups of *Acidovorax*.
70

71 **Material and methods**

72 **Origin of strains and genomes**

73 Fifty-two strains of endophytic *Acidovorax* were isolated from the root systems of healthy *Lotus*
74 *japonicus* ecotype Gifu B-129 *(*subsequently called *L. japonicus)* grown in natural soil in
75 Cologne, Germany. DNA from all strains was extracted and sequenced using an Illumina HiSeq
76 2500 device (Illumina, USA). The isolation and sequencing procedure is described in detail
77 elsewhere [14]. Genomes assemblies are available in the European Nucleotide Archive under
78 the accession number PRJEB37696.
79 In addition, 54 other genomes where obtained from NCBI. The collection includes 15 species:
80 *A. anthurii*, *A. avenae*, *A. carolinensis*, *A. cattleyae*, *A. citrulli*, *A. delafieldii*, *A. defluvii*, *A.*
81 *ebreus*, *A. facilis*, *A. kalamii*, *A. konjaci*, *A. monticola*, *A. oryzae*, *A. radicis, A. varianellae* and
82 *A. spp*. According to the database, all the selected bacterial genomes originate from plant, soil
83 and water samples. Details on the selected genomes are summarized in Supplemental Material
84 1. The mean level of completion for all 106 genomes was calculated to 0.986.
85 Based on the available metadata, we assigned the genomes to 3 behavioural phenotypes: 62
86 genomes belong to commensal or beneficial plant-associated strains (thereby termed
87 “commensals”), 21 to plant pathogenic strains (thereby termed “pathogens”) and 23 to free-
88 living strains (thereby termed “free-living”). According to the results of our *in planta* bioassays
89 (see below), we further classified the *Lotus*-isolated strains by their ability to promote *Lotus*
90 *japonicus* growth.
91

92 **Linear discriminant analysis effect sizes**

93 We studied genomic features across the strains isolated from *L. japonicus* and correlated the
94 obtained data with the effects detected by the *in planta* bioassays (see below). Therefore, we
95 annotated the genomes using Anvi'o 6.2 microbial multi-omics platform [15] which computes *k*-
96 mer frequencies and identifies coding sequences using Prodigal [16]. Afterwards, HMMER3 [17]
97 was used to profile the genomes with hidden Markov models and to find homologous protein
98 families in the Pfam database v33.1 [18]. Using the features occurrence frequency matrix
99 generated by Anvi'o 6.2, we calculated the effect sizes of the features over a linear discriminant
100 analysis (LEfSe [19]) between the groups of interest. We chose the default alpha values of 0.05
101 for the factorial Kruskal-Wallis test (KW) and the pairwise Wilcoxon test (W) and a threshold of
102 2.0 for the Linear Discriminant Analysis (LDA) logarithmic scores.
103

104 **Pan-genome analysis**

105 We used Anvi'o 6.2 further to pre-process the genomes and reconstruct *Acidovorax* pan-
106 genome [20]. We inferred the pan-genome with the following options: DIAMOND in sensitive
107 mode to calculate amino-acids sequences similarity, Minbit parameter to 0.5, minimum
108 occurrence of gene clusters to 2, MCL inflation parameter to 7. We separated gene clusters into
109 occurrence frequency classes. Kernel gene clusters were defined as present in 106 genomes.
110 Core gene clusters were defined as present in 100 to 105 genomes. Shell gene clusters were
111 defined as present in 16 to 99 genomes. Cloud gene clusters were defined as present in 2 to 15
112 genomes. Singleton gene clusters were defined as present in only 1 genome and were
113 excluded from the downstream processing to reduce computational load. We calculated
114 functional and geometrical homogeneity for each gene cluster and genome average nucleotide
115 identity using pyANI [21]. We calculated a functions occurrence frequency matrix and functions
116 enrichment scores for gene clusters' functions by assigning each gene cluster to the closest
117 Pfam.
118

119 **Comparative genomics**

120 We performed all downstream analysis in R (v4.02, code available on https://github.com/rsiani/
121 AVX_PGC). We calculated total length, GC%, number of genes, gene clusters and singleton
122 gene clusters, average gene length and number of genes per kb (gene density) for each of the
123 genomes. We assessed the significance of differences by Pairwise Student's t-test with Holm-
124 Bonferroni's correction for multiple testing ($p < 0.05$).
125 We converted the function frequency occurrence matrix (3036 Pfams) to a binary
126 presence/absence matrix and filtered zero variance (757 Pfams), near zero variance (1668
127 Pfams) and correlated variables (0 Pfams) to remove redundancy (resulting in 1368 Pfams). We
128 performed a Principal Component Analysis (PCA, R package: "FactoMineR", v2.3) to ordinate
129 the strains based on their functional similarity and tested the significance of the clustering by
130 PERMANOVA (package: "vegan", v2.5-7). We isolated the features responsible for most of the
131 variance explained by extracting the highest contributors for each of the first 3 components.
132 From the enriched feature profiles predicted by Anvi'o 6,2, we manually curated a list of
133 features putatively correlated with plant-association. Enrichment score and adjusted
134 significance value were used to assess the relevance of the features across the groups.
135 We retrieved secondary metabolites biosynthesis gene clusters using AntiSMASH 5.0 [22]. We
136 launched a local instance of the program with no extra features at a "relaxed" strictness level,
137 running only the core detection modules. At this strictness level, well-defined clusters and
138 partial clusters are detected and annotated against the antiSMASH database.
139 We built a classification model using neural networks with feature extraction (R package "caret",
140 v6.0-86), a model employing a preliminary feature extraction step to reduce redundancy, while
141 preserving information and decreasing computational load [23]. We trained the model over 90
142 % of the strains with "leave-one-out" cross-validation over 1000 repeats, using accuracy scores
143 to select the optimal parameters. The fit of the model was evaluated by predicting labels for the
144 remaining 10 % of the strains and again against the whole dataset Results were assessed by
145 calculating confusions matrix for both predictions.
146
147 ***In planta* bioassays**

148 We prepared seeds of *L. japonicus* by sandpaper scarification and surface sterilization with a
149 10% DanKlorix Original (CP GABA GmbH, Germany) and 0.1% sodium dodecyl sulfate (SDS)
150 solution. We germinated the seeds on a 0,8 % water-agar plate for 3 days at 22 °C in the dark
151 followed by 4 days at 22 °C in the light at 210 µM/m²s intensity (growth cabinet PK 520-LED,
152 Polyklima).
153 We transferred plantlets to pots (Göttinger 7 x 7 x 8 cm, Hermann Meyer KG, Germany) filled
154 with washed and autoclave sterilized quartz-sand (Casafino Quarzsand, fire-dried, 0,7 – 1,2
155 mm, BayWa AG, Germany) at a density of 5 plants per pot. Pots were supplied with a thin layer
156 of synthetic cotton at the bottom to prevent the sand running out through the holes.
157 44 of the *Acidovorax* strains isolated from healthy *L. japonicus* plants were individually pre-
158 grown in 50 % TSB media at 30°C overnight and diluted to an OD_{600} of 0,001 using 1/3 BNS-
159 AM medium (Basal Nutrient Solution [24] modified for arbuscular mycorrhiza (0.025 mM
160 KH_2PO_4)). 25 ml of this bacterial suspension was applied to the pots. Finally, 20 ml of the sterile
161 1/3 BNS-AM-bacterial solution was added. Plants were grown at 60 % air humidity and light
162 intensity of 150 µM/m^{2}s. The photo-period was set to 16 h light/ 8 h dark long day with a
163 temperature cycle of 24/22 °C. For each bacterial strain tested, four replicate pots were
164 prepared.
165 After 9 weeks of growth, we harvested the plants and determined root and shoot length, wet
166 weight and dry weight after freeze drying (Alpha 1-2, Martin Christ Gefriertrocknungsanlagen
167 GmbH, Germany). Statistical significance was assessed by Pairwise Student's *t*-test adjusted
168 for multiple comparisons using the Holm-Bonferroni method ($p < 0.05$).
169

170 **Results**

171 ***Acidovorax* strains isolated from healthy *L. japonicus* roots diversely affect their host**

172 We compared growth metrics of *L. japonicus* inoculated with different strains to evaluate the
173 outcomes of the plant-association. Overall, 34 out of 44 tested strains showed significant effects
174 ($p < 0.05$; Figure 1) when considering all the collected measurements of plants' growth (n = 25).
175 Twenty-one strains displayed a positive effect on at least one metric. Nine strains displayed a

176 negative effect on plant growth, markedly on fresh weight measurements. Four strains
177 displayed contrasting effects on different metrics and 10 had no significant effect on growth.
178 From the 21 strains that resulted in improved plant-growth, 7 strains displayed a more
179 consistent effect across all the replicates on at least one of the considered metrics ($p < 0.001$).
180 We selected these robust growth-promoters for a follow-up genomics comparison.
181

182 **Nineteen Pfams discriminate the robust plant growth-promoting *Acidovorax* strains**

183 To isolate genomic differences correlated with the outcomes of the *in planta* bioassays, we
184 calculated linear discriminant analysis effect sizes on the function occurrence frequency table
185 and identified 19 Pfams discriminating the 7 robust growth-promoters from the remainder of the
186 *Lotus*-isolated strains (KW $p < 0.05$, W $p < 0.05$, logarithmic LDA score > 2.0, Figure 2; Table
187 1). Out of those, 15 Pfams were enriched in the genomes of robust growth-promoters, related to
188 4 broad functional categories: chemotaxis by sensing and uptake of organic acids and sugars
189 (tripartite tricarboxylate transporters, TTTs, and periplasmic binding proteins, PBPs),
190 colonization through synthesis and detoxification of plant secondary metabolites (aldolase, aldo-
191 keto reductase, rhodanase, amidase and mannosyltransferase), competition by synthesis,
192 secretion and detoxification of antimicrobial compounds (beta-lactamase, polyketide cyclase,
193 tetrapyrrole corrin-porphyrin methlyase, dynein-related domain and dienelactone hydrolase) and
194 transcriptional regulation (FCD domain, IclR domain and sigma 70 factor). We found 4 Pfams
195 which were less abundant in the genomes of robust growth-promoters, also implicated in
196 chemotaxis (Tripartite ATP-independent periplasmic transporters, TRAPs), colonization (FliO
197 and the FG-GAP repeat) and regulation (metallo-peptidase M90).
198

199 ***Acidovorax* has an open pan-genome**

200 We reconstructed the *Acidovorax* pan-genome from 106 genomes (Figure 3), representing 15
201 out of the 23 classified *Acidovorax* species [51], along with several yet unclassified strains, and
202 capturing a large share of the genomic variability in the genus. The pan-genome contains a total
203 of 523555 genes grouped in 34146 gene clusters, of which 2 % belonged to the kernel (present

204 in all of the genomes), 3% belonged to the core (present in 100 to 105 genomes), 13%
205 belonged to the shell (present in 16 to 99 of the genomes), 45 % belonged to the cloud (present
206 in 2 to 15 genomes) and 37 % were singleton (present in one genome only). Ninety-five percent
207 of the gene clusters were classified as accessory, while 5 % are shared by all or most of the
208 genomes. By fitting our results to a Heaps' Power-law regression model [52] we obtained a $\gamma <$
209 1 of 0.48, which defines *Acidovorax* pan-genome as "open", with positive rates of novel genes
210 discovery for every additional genome included.
211

212 **Pathogenic *Acidovorax* strains have longer genomes but less genes**

213 We calculated total length, GC%, number of genes, gene clusters and singleton gene clusters,
214 average gene length and number of genes per kb (gene density) for each of the genomes
215 (Figure 4a, Supplemental Material 2). On average pathogens had longer genomes (5.38 mb,
216 SD = 0.27) than commensals (5.21 mb, SD = 1.03, $p < 0.01$) and free-living (4.72 mb, SD =
217 0.53, $p < 0.0001$, Figure 4b). However, when testing for differences in gene density, pathogens
218 had less genes per kb (0.86, SD = 0.09) than both commensals (1.01, SD = 0.05, $p < 0.0001$)
219 and free-living (0.94, SD = 0.03, $p < 0.001$, Figure 4c).
220

221 **Strains separate according to behavioural phenotype**

222 We performed a PCA on the function presence/absence matrix and found that the first 3
223 dimensions explained 47 % of the variance in the matrix (24.3 %, 12.4 % and 10.3 %). The
224 individual strains clustered according to their observed behavioural phenotype ($p < 0.05$), with
225 pathogens grouping in a neatly separated cluster and a partial overlap between free-living and
226 commensal strains (Figure 5ab). Notably, no clustering was visible when considering the
227 original habitat of the strains. We extracted the highest contributing variables for the first 3
228 components (Figure 5c, Table 2).
229 This approach retrieved a total of 14 Pfams displaying a strong variance across the groups.
230 Two of these, the C-terminal domain of a secreted lipases and the mutagenesis inducer HIM1,
231 contributed the most to the first component and were found in all of the commensals, 35 % of

232 the free-living and none of the pathogens. A third Pfam, characterized by a WG repeat motif,
233 was only retrieved in 40 % of the commensals and accounted for a high proportion of the
234 second component explanatory power. Finally, the highest contributor to the third component
235 was a putative genomic island, encoding 11 elements of the type VI secretion-system, present
236 in 95 % of the pathogens, 61 % of the commensals and only 13 % of the free-living strains.
237

238 **Pathogenic and commensal *Acidovorax* strains have a distinctive set of features**

239 We performed a function enrichment analysis to isolate features unique or more represented in
240 the different groups (Supplemental Material 3). 1243 out of 3036 Pfams were significantly
241 enriched in 1 or 2 groups (adjusted $q < 0.05$). We further investigated enriched functions from
242 plant-associated strains only: 371 Pfams strongly associated with commensals ($q < 0.05$) and
243 303 Pfams strongly associated with pathogens ($q < 0.05$) (Figure 6a). From these, we manually
244 curated a list of 54 features (Table 3) putatively involved in plant-microbe and microbe-microbe
245 interactions (Figure 6b). We assigned them to 4 families based on known performed function:
246 22 effectors, 13 hydrolytic enzymes , 12 motility functions and 7 secondary metabolites .
247 Eighteen effectors and known virulence factors were enriched in pathogens, among which,
248 notably, members of the HrpB gene of the type III secretion system, and its regulatory element
249 HpaP. Four effectors were also identified in commensals, including a type II secretion-system
250 protein.
251 Among the hydrolytic enzymes, 9 different Pfams were found to be enriched in pathogens, all
252 related to plant and fungal polysaccharides degradation, including components of pectate
253 lyases, amylases, chitinases, cellulases and glucanases. Four hydrolytic enzymes Pfams were
254 enriched in commensals, but mainly responsible for the degradation of complex bioactive
255 compounds, such as flavonoids, chlorophyll and aromatic-ring backbones.
256 Interestingly, 10 Pfams related to diverse motility structures, namely flagella and pili, and
257 chemotaxis were predominantly found in commensals. For comparison, just 2 motility related
258 Pfams were enriched in pathogens.

259 Among those enriched in commensals, we also found 6 Pfams related to bacterial cellulose
260 biosynthesis and 1 polyketide-synthetase Pfams enriched in pathogens.
261 Using AntiSMASH 5.0, we retrieved a repertoire of 15 biosynthesis gene clusters (BGCs)
262 among the bacterial genomes (Figure 7). The most commonly retrieved BGCs were those for
263 bacteriocin and terpene production. Interestingly, phosphonate and all non-ribosomal peptide-
264 synthetase BGCs (NRPS, NRPS-like, NRPS-T1PKS) were almost unique to pathogens and
265 retrieved in more than half of the pathogenic strains.
266

267 **Genotypes can predict the behaviour of the strains**

268 We tested whether a model could predict a strain behavioural phenotype from its gene
269 repertoire. We trained a neural network with feature extraction classifier on the gene function's
270 presence/absence profiles of 90% of our strains (n = 96). The optimal model, which we selected
271 according to accuracy value, registered a mean balanced accuracy = 0.93 and an area under
272 the curve (AUC) = 0.97, with the selected final values of size = 3 and decay = 0.1. We tested
273 the predictive power of the model against the remainder 10% of the strains (n = 10) and
274 registered accuracy = 1, sensitivity = 1, specificity = 1, kappa = 1, 95% confidence interval =
275 0.69 to 1 and p = 0.006. When testing against the whole collection (n = 106), all metrics
276 remained unchanged but for the 95% confidence interval = 0.97 to 1 and p = 2.2e-16.
277

278 **Discussion**

279 **Robust growth-promoting strains share traits which allow a better use of phytochemicals**

280 Our *in planta* bioassays showed a wide range of effects associated with the presence of diverse
281 *Acidovorax* isolates obtained from healthy roots of *L. japonicus*. We compared the genomes of
282 7 robust growth-promoters against the remainder of the isolates and retrieved 19 discriminant
283 Pfams related to different aspects of plant-microbe and microbe-microbe interactions:
284 chemotaxis towards root exudates, metabolism of plant secondary metabolites, antagonistic
285 competition and transcriptional regulation.

286 Organic acids are a major component of root exudates [110]. Microbial transporters, such as
287 ABC-type transport systems, TRAPs and TTTs, are essential to make use of these carbon rich
288 compounds and a number of studies confirmed that their presence is correlated to improved
289 colonization in both plant-growth promoters [111] and pathogens [32]. Many transporters are
290 highly specific for individual substrates. For example, TTTs, which are enriched in robust-growth
291 promoters in our study, show a higher affinity towards citrate compared to TRAPs. As shown by
292 metabolic profiling [112], citrate is more abundant than other organic acids in *L. japonicus* root
293 tissue and improved sensing and uptake of citrate could translate in an evolutionary advantage
294 of microbiota towards the colonization of this plant. Our robust growth-promoters also shared an
295 enrichment of several features related to the metabolism of various plant-derived compounds,
296 such as benzoic acids, carbonyls, cyanide and rare sugars. Some of these traits have been
297 already correlated to improved plant-association in taxonomically diverse bacteria [13, 113,
298 114]. Furthermore, we observed the enrichment of an amidase involved in the biosynthesis of
299 indole-3-acetic acid and of a known regulator of GABA uptake [115]. The role of auxin in plant-
300 growth promotion by bacteria has been thoroughly characterized [116] and GABA has been
301 more recently discovered to act as signal from plants to their associated microbiota [117, 118].
302 Finally, we found enriched components of diverse regulatory pathways and of both antibiotic
303 synthesis and degradation, which could help the robust growth-promoters to not only better
304 colonize the plant by degrading plant-derived phytochemicals with antimicrobial properties, but
305 also to gain competitive advantage over other microbial populations.
306 Overall, we found evidence of genomic differences among robust growth-promoting bacteria
307 and the remainder of *Acidovorax* isolates, suggesting improved chemotaxis, competitive traits
308 and interaction with the plant metabolism and hormonal balance, possibly leading to a stronger
309 association between host and colonizers and explaining the better growth outcomes observed
310 *in planta*.
311

312 **The evolutionary trajectory towards pathogenic plant-association**

313 *Acidovorax* strains are naturally found to occupy widely diverse niches. In the frame of this
314 study, we reconstructed their pan-genome to explore the importance of genomic features
315 across the whole behavioural spectrum. Pan-genome analyses have become a staple to
316 estimate the complete gene repertoire accessible to an organism and to understand genotype
317 variations and evolution in a broader context [119, 120]. We found that the *Acidovorax* pan-
318 genome is largely made up by accessory or unique gene clusters (95 %) and predisposed to a
319 continuous inflation, a predictive feature of functionally flexible organisms [121], with each
320 occupied niche being a potential source of novel genomic traits.
321 Specialization has been associated with smaller genomes and previously reported in
322 pathogenic strains [121, 122]. Therefore, we studied *Acidovorax* genome size and density,
323 expecting to observe evidence of reductive evolution. For example, Merhej and colleagues
324 analysed a comprehensive collection of 317 bacterial genomes to trace the evolutionary path
325 from free-living to specialized intracellular strains [123], uncovering "massive gene loss" as a
326 consequence of more gene loss than horizontal gene transfer (HGT) events. Mainly in isolated
327 niches like the interior of roots, HGT rates are considered as low due to the missing interaction
328 with other microbiota. Surprisingly, in our study, the genomes of pathogenic *Acidovorax* were
329 the largest, yet showed a significantly lower gene density than both free-living and commensals
330 strains. Similar data was also observed for *Rickettsia prowazekii* [124], which features more
331 non-coding sequences than any of its close, non-pathogenic, relatives. In their review on
332 pathogenomics, Georgiades and Raoult argued that true bacterial speciation is only observed in
333 the contest of segregated niche, such in the case of obligated parasitism [125]. For Acidovorax,
334 Fegan [10] listed 28 known Graminaceae hosts for *Acidovorax avenae* subsp. a*venae* and 10
335 Cucurbitaceae natural hosts and 2 Solenaceae for *Acidovorax avenae* subsp. c*itrulli*. Thus,
336 *Acidovorax* pathogens seems still far from true speciation, as suggested by their wide choice of
337 hosts, and, likely, have already endured evolutionary driven gene losses, whereas extensive
338 genome reductions still have to occur.
339
340 **Major functional differences across the groups**

341 Principal component analysis revealed that pathogens differ in their genomes from commensal
342 and free-living strains. Among the differences that contributed the most to the separation, we
343 found that the lipase C-terminal domain and the mutagenesis inducer HIM1 were both enriched
344 in commensal strains. Assis and colleagues investigated the phylogeny of lipases in bacteria
345 and found orthologous of the same secreted lipase ubiquitous among plant-associated strains,
346 including *Acidovorax* [126]. Pathogens may be less dependent on lipases, as, during infection,
347 plant-derived lipids may be of minor value to them, as they preferentially hydrolyse
348 carbohydrates to cover their nutritional needs.
349 The presence of type VI secretion-systems has been strongly correlated with plant-association
350 in Gram-negative bacteria [127] and has been in observed in pathogenic and commensal
351 strains alike. Similarly, in *Acidovorax*, we retrieved a putative type VI secretion-system genomic
352 island in both groups of plant-associated bacteria (commensals and pathogens, but only in 13
353 % of the free-living strains). For the pathogens, we also identified an operon encoding
354 components of the type III secretion-system, absent from the other groups.
355 The distribution of these Pfams across the groups suggests the recruitment of commensals
356 from the larger pool of free-living strains through horizontal gene transfer of a single genomic
357 island encoding elements of the type VI secretion-system and further specialization of
358 commensals into pathogenic strains, through gene losses and acquisition of type III secretion-
359 systems.
360 We observed in the commensals an enrichment of several motility-associated domains. Pallen
361 and Wren [128] postulated the loss of motility as a common side-effect of intracellular
362 endosymbiosis, a phenomena recently witnessed in several emerging pathogens. It stands to
363 be clarified whether this adaptation occurs for disuse, to prevent recognition by the host
364 immune system or both. For commensals however, which are depending on chemotaxis to
365 make use of the plant-derived phytochemicals, motility is an essential function.
366 Finally, pathogens showed an enrichment of polyketide synthases and non-ribosomal peptide
367 synthases, which have been both extensively researched due to their promising role in
368 pharmaceutical applications for the production of diverse antimicrobial, immunosuppressive and

369 cytostatic compounds [129, 130]. Pathogenic *Acidovorax*, thus, have access to a wider array of
370 secondary metabolites, likely necessary for microbe-microbe competition [131] and possibly to
371 interact with the host.
372

373 **Conclusions**

374 The focus of this research study has been to assess the role of genomic traits across the
375 *Acidovorax* behavioural spectrum and to evaluate which genomic features can discriminate
376 plant-pathogenic from commensal and plant-growth promoting strains. We have reported many
377 discriminant traits through association of plant growth data with *in silico* pan-genome-wide
378 comparisons. The robustness of our analysis was also supported by our neural network
379 classifier, which accurately matched each individual to its observed phenotype by using the
380 information encoded in the pan-genome, validating our hypothesis. Researchers in the field of
381 genomics and microbiology have been investigating the potential of machine learning
382 applications to extract meaningful patterns from the high-dimensional data generated by Next-
383 Generation Sequencing [132, 133, 134, 135]. Even though our method was tested on a single
384 genus, it shows promises for generalization and the advancement of genotype-based, high-
385 throughput phenotyping and monitoring of emerging pathogens.
386 However, our data is based on genomic predictions and the importance of the described Pfams,
387 both for plant-growth promoting commensals as well as plant-pathogens, needs to be verified
388 firstly by analysing bacterial transcriptomes during the interaction with the plant, followed by
389 targeted mutagenesis and analysis of the impact of bacterial mutants on survival in the
390 rhizosphere and plant growth.
391

392 **Authors statement**

393 The authors declare no financial conflicts of interest.
394

395 **Acknowledgement**

396 Michael Schloter and Caroline Gutjahr were supported by grants from the Deutsche
397 Forschungsgemeinschaft [DFG; SCHL446/38-1 and GU1423/3-1] respectively the frame of the
398 SPP2125 “Deconstruction and reconstruction of the plant microbiota [DECRyPT]”. We thank
399 Ruben Garrido-Oter for making the isolates available for the *L. japonicus* bioassays and the
400 respective sequenced genomes for the genomics comparison We highly appreciate the
401 discussions with Martin Parniske and Corinna Dawid. We thank M.H.H. Nguyen for help with
402 the *L. japonicus* bioassays.

403 **Bibliography**

404 1. Harbort CJ, Hashimoto M, Inoue H, Niu Y, Guan R, et al. Root-Secreted Coumarins and the
405 Microbiota Interact to Improve Iron Nutrition in Arabidopsis. Cell Host Microbe 2020;28:825-
406 837.e6. doi: 10.1016/j.chom.2020.09.006

407 2. Finkel OM, Salas-González I, Castrillo G, Conway JM, Law TF, et al. A single bacterial genus
408 maintains root growth in a complex microbiome. Nature 2020;587:103–108. doi: 10.1038/s41586-
409 020-2778-7

410 3. Berg G, Grube M, Schloter M, Smalla K. The plant microbiome and its importance for plant and
411 human health. Front Microbiol 2014;5:1. doi: 10.3389/fmicb.2014.00491

412 4. Durán P, Thiergart T, Garrido-Oter R, Agler M, Kemen E, et al. Microbial Interkingdom
413 Interactions in Roots Promote Arabidopsis Survival. Cell 2018;175:973-983.e14. doi:
414 10.1016/j.cell.2018.10.020

415 5. Rodriguez PA, Rothballer M, Chowdhury SP, Nussbaumer T, Gutjahr C, et al. Systems Biology
416 of Plant-Microbiome Interactions. Mol Plant 2019;12:804–821. doi: 10.1016/j.molp.2019.05.006

417 6. Idnurm A, Howlett BJ. Analysis of loss of pathogenicity mutants reveals that repeat-induced
418 point mutations can occur in the Dothideomycete Leptosphaeria maculans. Fungal Genet Biol
419 2003;39:31–37. doi: 10.1016/S1087-1845(02)00588-1

420 7. Kanda A, Ohnishi S, Tomiyama H, Hasegawa H, Yasukohchi M, et al. Type III secretion
421 machinery-deficient mutants of Ralstonia solanacearum lose their ability to colonize resulting in
422 loss of pathogenicity. J Gen Plant Pathol 2003;69:250–257. doi: 10.1016/S1087-1845(02)00588-1

423 8. Melnyk RA, Hossain SS, Haney CH. Convergent gain and loss of genomic islands drive lifestyle
424 changes in plant-associated Pseudomonas. ISME J 2019;13:1575–1588. doi: 10.1016/S1087-
425 1845(02)00588-1
426 9. Willems A, Gillis M. Acidovorax . In: Bergey's Manual of Systematics of Archaea and Bacteria.
427 John Wiley & Sons, Ltd; 2015. pp. 1–16. doi: 10.1099/00207713-42-1-107
428 10. Fegan M. Plant pathogenic members of the genera Acidovorax and Herbaspirillum. In: Plant-
429 Associated Bacteria. Springer Netherlands; 2006. pp. 671–702. doi: 10.1007/978-1-4020-4538-
430 7_18
431 11. Giordano PR, Chaves AM, Mitkowski NA, Vargas JM. Identification, characterization, and
432 distribution of Acidovorax avenae subsp. avenae associated with creeping bentgrass etiolation
433 and decline. Plant Dis 2012;96:1736–1742. doi: 10.1007/978-1-4020-4538-7_18
434 12. Han S, Li D, Trost E, Mayer KF, Corina V, et al. Systemic responses of barley to the 3-
435 hydroxy-decanoyl-homoserine lactone producing plant beneficial endophyte acidovorax radicis
436 N35. Front Plant Sci 2016;7:1868. doi: 10.3389/fpls.2016.01868
437 13. Levy A, Salas Gonzalez I, Mittelviefhaus M, Clingenpeel S, Herrera Paredes S, et al. Genomic
438 features of bacterial adaptation to plants. Nat Genet 2018;50:138–150. doi: 10.1038/s41588-017-
439 0012-9
440 14. Wippel K, Tao K, Niu Y, Zgadzaj R, Guan R, et al. Host preference and invasiveness of
441 commensals in the Lotus and Arabidopsis root microbiota. BioRxiv 2021;2021.01.12.426357. doi:
442 10.1101/2021.01.12.426357
443 15. Eren AM, Esen OC, Quince C, Vineis JH, Morrison HG, et al. Anvi'o: An advanced analysis
444 and visualization platformfor 'omics data. PeerJ 2015;2015:e1319. doi: 10.7717/peerj.1319
445 16. Hyatt D, Chen GL, LoCascio PF, Land ML, Larimer FW, et al. Prodigal: Prokaryotic gene
446 recognition and translation initiation site identification. BMC Bioinformatics 2010;11:119. doi:
447 10.1186/1471-2105-11-119
448 17. Eddy SR. A new generation of homology search tools based on probabilistic inference.
449 Genome Inform 2009;23:205–211. doi: 10.1142/9781848165632_0019

450 18. El-Gebali S, Mistry J, Bateman A, Eddy SR, Luciani A, et al. The Pfam protein families
451 database in 2019. Nucleic Acids Res 2019;47:D427–D432. doi: 10.1093/nar/gky995
452 19. Segata N, Izard J, Waldron L, Gevers D, Miropolsky L, et al. Metagenomic biomarker
453 discovery and explanation. Genome Biol 2011;12:R60. doi: 10.1186/gb-2011-12-6-r60
454 20. Delmont TO, Eren EM. Linking pangenomes and metagenomes: The Prochlorococcus
455 metapangenome. PeerJ 2018;2018:e4320. doi: 10.7717/peerj.4320
456 21. Pritchard L, Cock P, Esen Ö. pyani v0.2.8: average nucleotide identity (ANI) and related
457 measures for whole genome comparisons. Epub ahead of print 5 March 2019. doi:
458 10.5281/ZENODO.2584238.
459 22. Blin K, Shaw S, Steinke K, Villebro R, Ziemert N, et al. antiSMASH 5.0: updates to the
460 secondary metabolite genome mining pipeline. Nucleic Acids Res 2019;47:W81–W87. doi:
461 10.1093/nar/gkz310
462 23. Khalid S, Khalil T, Nasreen S. A survey of feature selection and feature extraction techniques
463 in machine learning. In: Proceedings of 2014 Science and Information Conference, SAI 2014.
464 Institute of Electrical and Electronics Engineers Inc.; 2014. pp. 372–378. doi:
465 10.1109/SAI.2014.6918213
466 24. Conn SJ, Hocking B, Dayod M, Xu B, Athman A, et al. Protocol: Optimising hydroponic growth
467 systems for nutritional and physiological analysis of Arabidopsis thaliana and other plants. Plant
468 Methods 2013;9:1–11. doi: 10.1186/1746-4811-9-4
469 25. Kelly DJ, Thomas GH. The tripartite ATP-independent periplasmic (TRAP) transporters of
470 bacteria and archaea. FEMS Microbiol Rev 2001;25:405–424. doi: 10.1111/j.1574-
471 6976.2001.tb00584.x
472 26. Simpson DA, Ramphal R, Lory S. Characterization of Pseudomonas aeruginosa fliO, a gene
473 involved in flagellar biosynthesis and adherence. Infect Immun 1995;63:2950–2957. doi:
474 10.1128/iai.63.8.2950-2957.1995
475 27. Barker CS, Meshcheryakova I V., Kostyukova AS, Samatey FA. FliO Regulation of FliP in the
476 Formation of the Salmonella enterica Flagellum. PLoS Genet 2010;6:e1001143. doi:
477 10.1371/journal.pgen.1001143

478 28. Absalon C, Van Dellen K, Watnick PI. A Communal Bacterial Adhesin Anchors Biofilm and
479 Bystander Cells to Surfaces. PLoS Pathog 2011;7:e1002210. doi: 10.1371/journal.ppat.1002210
480 29. Göhler AK, Staab A, Gabor E, Homann K, Klang E, et al. Characterization of MtfA, a novel
481 regulatory output signal protein of the glucose-phosphotransferase system in Escherichia coli K-
482 12. J Bacteriol 2012;194:1024–1035. doi: 10.1128/JB.06387-11
483 30. Xu Q, Göhler AK, Kosfeld A, Carlton D, Chiu HJ, et al. The structure of MLC titration factor a
484 (MtfA/YeeI) reveals a Prototypical zinc metallopeptidase related to anthrax lethal factor. J Bacteriol
485 2012;194:2987–2999. doi: 10.1128/JB.00038-12
486 31. Rosa LT, Bianconi ME, Thomas GH, Kelly DJ. Tripartite ATP-independent periplasmic (TRAP)
487 transporters and Tripartite Tricarboxylate Transporters (TTT): From uptake to pathogenicity.
488 Frontiers in Cellular and Infection Microbiology 2018;8:33. doi: 10.3389/fcimb.2018.00033
489 32. Cangelosi GA, Ankenbauer RG, Nestert EW. Sugars induce the Agrobacterium virulence
490 genes through a periplasmic binding protein and a transmembrane signal protein (crown
491 gapl/signal transduction/ChvE/VirA/galactose-binding proteins). 1990;87:6708-6712 doi:
492 http://www.jstor.org/stable/2355369.
493 33. Rodionova IA, Li X, Thiel V, Stolyar S, Stanton K, et al. Comparative genomics and functional
494 analysis of rhamnose catabolic pathways and regulons in bacteria. Front Microbiol 2013;4:407.
495 doi: 10.3389/fmicb.2013.00407
496 34. Yamauchi Y, Hasegawa A, Taninaka A, Mizutani M, Sugimoto Y. NADPH-dependent
497 reductases involved in the detoxification of reactive carbonyls in plants. J Biol Chem
498 2011;286:6999–7009. doi: 10.1074/jbc.M110.202226
499 35. Cipollone R, Ascenzi P, Tomao P, Imperi F, Visca P. Enzymatic detoxification of cyanide:
500 Clues from Pseudomonas aeruginosa rhodanese. J Mol Microbiol Biotechnol 2008;15:199–211.
501 doi: 10.1159/000121331
502 36. Pollmann S, Müller A, Weiler EW. Many Roads Lead to 'Auxin': of Nitrilases, Synthases, and
503 Amidases. Plant Biol 2006;8:326–333. doi: 10.1055/s-2006-924075

504 37. Lengeler KB, Tielker D, Ernst JF. Protein-O-mannosyltransferases in virulence and
505 development. Cellular and Molecular Life Sciences 2008;65:528–544. doi: 10.1007/s00018-007-
506 7409-z
507 38. Zowawi HM, Harris PNA, Roberts MJ, Tambyah PA, Schembri MA, et al. The emerging threat
508 of multidrug-resistant Gram-negative bacteria in urology. Nat Rev Urol 2015;12:570–584. doi:
509 10.1038/nrurol.2015.199
510 39. van den Bosch TJM, Tan K, Joachimiak A, Welte CU. Functional profiling and crystal
511 structures of isothiocyanate hydrolases found in gut-associated and plant-pathogenic bacteria.
512 Appl Environ Microbiol 2018;84:2020. doi: 10.1128/AEM.00478-18
513 40. Sultana A, Kallio P, Jansson A, Wang JS, Niemi J, et al. Structure of the polyketide cyclase
514 SnoaL reveals a novel mechanism for enzymatic aldol condensation. EMBO J 2004;23:1911–
515 1921. doi: 10.1038/sj.emboj.7600201
516 41. Raux E, Schubert HL, Warren MJ. Biosynthesis of cobalamin (vitamin B12): A bacterial
517 conundrum. 2000. Epub ahead of print 2000. doi: 10.1007/PL00000670.
518 42. Schoenhofen IC, Li G, Strozen TG, Howard SP. Purification and characterization of the N-
519 terminal domain of ExeA: A novel ATPase involved in the type II secretion pathway of Aeromonas
520 hydrophila. J Bacteriol 2005;187:6370–6378. doi: 10.1128/JB.187.18.6370-6378.2005
521 43. Schlomann M, Schmidt E, Knackmuss HJ. Different types of dienelactone hydrolase in 4-
522 fluorobenzoate-utilizing bacteria. J Bacteriol 1990;172:5112–5118. doi: 10.1128/jb.172.9.5112-
523 5118.1990
524 44. Schlomann M, Ngai KL, Ornston LN, Knackmuss HJ. Dienelactone hydrolase from
525 Pseudomonas cepacia. J Bacteriol 1993;175:2994–3001. doi: 10.1128/jb.175.10.2994-3001.1993
526 45. Lord DM, Uzgoren Baran A, Soo VWC, Wood TK, Peti W, et al. McbR/YncC: Implications for
527 the mechanism of ligand and DNA binding by a bacterial gntr transcriptional regulator involved in
528 biofilm formation. Biochemistry 2014;53:7223–7231. doi: 10.1021/bi500871a
529 46. Planamente S, Mondy S, Hommais F, Vigouroux A, Moréra S, et al. Structural basis for
530 selective GABA binding in bacterial pathogens. Mol Microbiol 2012;86:1085–1099. doi:
531 10.1111/mmi.12043

532 47. Thomson NR, Nasser W, McGowan S, Sebaihia M, Salmond GPC. Erwinia carotovora has two
533 KdgR-like proteins belonging to the IclR family of transcriptional regulators: Identification and
534 characterization of the RexZ activator and the KdgR repressor of pathogenesis. Microbiology
535 1999;145:1531–1545. doi: 10.1099/13500872-145-7-1531
536 48. Molina-Henares AJ, Krell T, Eugenia Guazzaroni M, Segura A, Ramos JL. Members of the
537 IclR family of bacterial transcriptional regulators function as activatorsand/or repressors. FEMS
538 Microbiology Reviews 2006;30:157–186. doi: 10.1111/j.1574-6976.2005.00008.x
539 49. Paget MSB, Helmann JD. The σ70 family of sigma factors. Genome Biology 2003;4:203. doi:
540 10.1186/gb-2003-4-1-203
541 50. Kazmierczak MJ, Wiedmann M, Boor KJ. Alternative Sigma Factors and Their Roles in
542 Bacterial Virulence. Microbiol Mol Biol Rev 2005;69:527–543. doi: 10.1128/mmbr.69.4.527-
543 543.2005
544 51. https://www.ncbi.nlm.nih.gov/taxonomy
545 52. Tettelin H, Riley D, Cattuto C, Medini D. Comparative genomics: the bacterial pan-genome.
546 Current Opinion in Microbiology 2008;11:472–477. doi: 10.1016/j.mib.2008.09.006
547 53. Chen CKM, Lee GC, Ko TP, Guo RT, Huang LM, et al. Structure of the
548 Alkalohyperthermophilic Archaeoglobus fulgidus Lipase Contains a Unique C-Terminal Domain
549 Essential for Long-Chain Substrate Binding. J Mol Biol 2009;390:672–685. doi:
550 10.1016/j.jmb.2009.05.017
551 54. Flaugnatti N, Le TTH, Canaan S, Aschtgen MS, Nguyen VS, et al. A phospholipase A1
552 antibacterial Type VI secretion effector interacts directly with the C-terminal domain of the VgrG
553 spike protein for delivery. Mol Microbiol 2016;99:1099–1118. doi: 10.1111/mmi.13292
554 55. Kelberg EP, Kovaltsova S V., Alekseev SY, Fedorova I V., Gracheva LM, et al. HIM1, a new
555 yeast Saccharomyces cerevisiae gene playing a role in control of spontaneous and induced
556 mutagenesis. Mutat Res - Fundam Mol Mech Mutagen 2005;578:64–78. doi:
557 10.1016/j.mrfmmm.2005.03.003

558 56. Karlowski WM, Zielezinski A, Carrère J, Pontier D, Lagrange T, et al. Genome-wide
559 computational identification of WG/GW Argonaute-binding proteins in Arabidopsis. Nucleic Acids
560 Res 2010;38:4231–4245. doi: 10.1093/nar/gkq162
561 57. Filloux A, Hachani A, Bleves S. The bacterial type VI secretion machine: yet another player for
562 protein transport across membranes. Microbiology 2008;154:1570–1583. doi:
563 10.1099/mic.0.2008/016840-0
564 58. Kapitein N, Bönemann G, Pietrosiuk A, Seyffer F, Hausser I, et al. ClpV recycles VipA/VipB
565 tubules and prevents non-productive tubule formation to ensure efficient type VI protein secretion.
566 Mol Microbiol 2013;87:1013–1028. doi: 10.1111/mmi.12147
567 59. English G, Byron O, Cianfanelli FR, Prescott AR, Coulthurst SJ. Biochemical analysis of TssK,
568 a core component of the bacterial Type VI secretion system, reveals distinct oligomeric states of
569 TssK and identifies a TssK-TssFG subcomplex. Biochem J 2014;461:291–304. doi:
570 10.1042/BJ20131426
571 60. Bingle LE, Bailey CM, Pallen MJ. Type VI secretion: a beginner's guide. Current Opinion in
572 Microbiology 2008;11:3–8. doi: 10.1016/j.mib.2008.01.006
573 61. Mintz KP, Fives-Taylor PM. impA, a gene coding for an inner membrane protein, influences
574 colonial morphology of Actinobacillus actinomycetemcomitans. Infect Immun 2000;68:6580–6586.
575 doi: 10.1128/IAI.68.12.6580-6586.2000
576 62. Suarez G, Sierra JC, Sha J, Wang S, Erova TE, et al. Molecular characterization of a
577 functional type VI secretion system from a clinical isolate of Aeromonas hydrophila. Microb Pathog
578 2008;44:344–361. doi: 10.1016/j.micpath.2007.10.005
579 63. Bladergroen MR, Badelt K, Spaink HP. Infection-blocking genes of a symbiotic Rhizobium
580 leguminosarum strain that are involved in temperature-dependent protein secretion. Mol Plant-
581 Microbe Interact 2003;16:53–64. doi: 10.1094/MPMI.2003.16.1.53
582 63. Zhou Y, Tao J, Yu H, Ni J, Zeng L, et al. Hcp family proteins secreted via the type VI secretion
583 system coordinately regulate Escherichia coli K1 interaction with human brain microvascular
584 endothelial cells. Infect Immun 2012;80:1243–1251. doi: 10.1128/IAI.05994-11

585 64. Cunnac S, Boucher C, Genin S. Characterization of the cis-Acting Regulatory Element
586 Controlling HrpB-Mediated Activation of the Type III Secretion System and Effector Genes in
587 Ralstonia solanacearum. J Bacteriol 2004;186:2309–2318. doi: 10.1128/JB.186.8.2309-2318.2004
588 65. Furutani A, Takaoka M, Sanada H, Noguchi Y, Oku T, et al. Identification of novel type III
589 secretion effectors in Xanthomonas oryzae pv. oryzae. Mol Plant-Microbe Interact 2009;22:96–
590 106. doi: 10.1094/MPMI-22-1-0096
591 66. van Gijsegem F, Gough C, Zischek C, Niqueux E, Arlat M, et al. The hrp gene locus of
592 Pseudomonas solanacearum, which controls the production of a type III secretion system,
593 encodes eight proteins related to components of the bacterial flagellar biogenesis complex. Mol
594 Microbiol 1995;15:1095–1114. doi: 10.1111/j.1365-2958.1995.tb02284.x
595 67. Baruch K, Gur-Arie L, Nadler C, Koby S, Yerushalmi G, et al. Metalloprotease type III effectors
596 that specifically cleave JNK and NF-κB. EMBO J 2011;30:221–231. doi: 10.1038/emboj.2010.297
597 68. Zhang H, Gao ZQ, Wang WJ, Liu GF, Xu JH, et al. Structure of the type vi effector-immunity
598 complex (Tae4-Tai4) provides novel insights into the inhibition mechanism of the effector by its
599 immunity protein. J Biol Chem 2013;288:5928–5939. doi: 10.1074/jbc.M112.434357
600 69. López-Lara IM, Kafetzopoulos D, Spaink HP, Thomas-Oates JE. Rhizobial NodL O-acetyl
601 transferase and nodS N-methyl transferase functionally interfere in production of modified nod
602 factors. J Bacteriol 2001;183:3408–3416. doi: 10.1128/JB.183.11.3408-3416.2001
603 70. Müller MG, Moe NE, Richards PQ, Moe GR. Resistance of Neisseria meningitidis to human
604 serum depends on T and B cell stimulating protein B. Infect Immun 2015;83:1257–1264. doi:
605 10.1128/IAI.03134-14
606 71. Carr S, Walker D, James R, Kleanthous C, Hemmings AM. Inhibition of a ribosome-
607 inactivating ribonuclease: The crystal structure of the cytotoxic domain of colicin E3 in complex
608 with its immunity protein. Structure 2000;8:949–960. doi: 10.1016/S0969-2126(00)00186-6
609 72. Krishnan HB. NolX of Sinorhizobium fredii USDA257, a type III-secreted protein involved in
610 host range determination, is localized in the infection threads of cowpea (Vigna unguiculata [L.]
611 Walp) and soybean (Glycine max [L.] Merr.) nodules. J Bacteriol 2002;184:831–839. doi: 10.1128/
612 JB.184.3.831-839.2002

613 73. El Ghachi M, Bouhss A, Barreteau H, Touzé T, Auger G, et al. Colicin M exerts its bacteriolytic
614 effect via enzymatic degradation of undecaprenyl phosphate-linked peptidoglycan precursors. J
615 Biol Chem 2006;281:22761–22772. doi: 10.1074/jbc.M602834200
616 74. Hattori Y, Iwata K, Suzuki K, Uraji M, Ohta N, et al. Sequence characterization of the vir region
617 of a nopaline type Ti plasmid, pTi-SAKURA. Genes Genet Syst 2001;76:121–130. doi:
618 10.1266/ggs.76.121
619 75. Fields KA, Nilles ML, Cowan C, Straley SC. Virulence Role of V Antigen of Yersinia pestis at
620 the Bacterial Surface. Infect Immun 1999;67:5395–5408. doi: 0019-9567/99/$04.000
621 76. Zhang D, de Souza RF, Anantharaman V, Iyer LM, Aravind L. Polymorphic toxin systems:
622 Comprehensive characterization of trafficking modes, processing, mechanisms of action, immunity
623 and ecology using comparative genomics. Biol Direct;7. Epub ahead of print 25 June 2012. doi:
624 10.1186/1745-6150-7-18.
625 77. Patzer SI, Albrecht R, Braun V, Zeth K. Structural and mechanistic studies of pesticin, a
626 bacterial homolog of phage lysozymes. J Biol Chem 2012;287:23381–23396. doi:
627 10.1074/jbc.M112.362913
628 78. Guyon K, Balagué C, Roby D, Raffaele S. Secretome analysis reveals effector candidates
629 associated with broad host range necrotrophy in the fungal plant pathogen Sclerotinia
630 sclerotiorum. BMC Genomics 2014;15:1–19. doi: 10.1186/1471-2164-15-336
631 79. Korotkov K V., Sandkvist M, Hol WGJ. The type II secretion system: Biogenesis, molecular
632 architecture and mechanism. Nat Rev Microbiol 2012;10:336–351. doi: 10.1038/nrmicro2762
633 80. Lohrke SM, Nechaev S, Yang H, Severinov K, Jin SJ. Transcriptional activation of
634 Agrobacterium tumefaciens virulence gene promoters in Escherichia coli requires the A.
635 tumefaciens rpoA gene, encoding the alpha subunit of RNA polymerase. J Bacteriol
636 1999;181:4533–4539. doi: 10.1128/jb.181.15.4533-4539.1999
637 81. Kadioglu A, Weiser JN, Paton JC, Andrew PW. The role of Streptococcus pneumoniae
638 virulence factors in host respiratory colonization and disease. Nat Rev Microbiol 2008;6:288–301.
639 doi: 10.1038/nrmicro1871

640 82. Charkowski AO, Alfano JR, Preston G, Yuan J, He SY, et al. The Pseudomonas syringae pv.
641 tomato HrpW protein has domains similar to harpins and pectate lyases and can elicit the plant
642 hypersensitive response and bind to pectate. J Bacteriol 1998;180:5211–5217. doi:
643 10.1128/jb.180.19.5211-5217.1998
644 83. Kotrba P, Inui M, Yukawa H. Bacterial phosphotransferase system (PTS) in carbohydrate
645 uptake and control of carbon metabolism. Journal of Bioscience and Bioengineering 2001;92:502–
646 517. doi: 10.1016/S1389-1723(01)80308-X
647 84. Johnson PE, Joshi MD, Tomme P, Kilburn DG, McIntosh LP. Structure of the N-terminal
648 cellulose-binding domain of Cellulomonas fimi CenC determined by nuclear magnetic resonance
649 spectroscopy. Biochemistry 1996;35:14381–14394. doi: 10.1021/bi961612s
650 85. Larson SB, Greenwood A, Cascio D, Day J, McPherson A. Refined molecular structure of pig
651 pancreatic α-amylase at 2.1 Å resolution. J Mol Biol 1994;235:1560–1584. doi:
652 10.1006/jmbi.1994.1107
653 86. Rodríguez-Sanoja R, Oviedo N, Sánchez S. Microbial starch-binding domain. Current Opinion
654 in Microbiology 2005;8:260–267. doi: 10.1016/j.mib.2005.04.013
655 87. Gijzen M, Kuflu K, Qutob D, Chernys JT. A class I chitinase from soybean seed coat. J Exp
656 Bot 2001;52:2283–2289. doi: 10.1093/jexbot/52.365.2283
657 88. Itoh T, Hibi T, Suzuki F, Sugimoto I, Fujiwara A, et al. Crystal structure of chitinase ChiW from
658 Paenibacillus sp. str. FPU-7 reveals a novel type of bacterial cell-surface-expressed multi-modular
659 enzyme machinery. PLoS One;11. Epub ahead of print 1 December 2016. doi:
660 10.1371/journal.pone.0167310.
661 89. Py B, Isabelle BG, Haiech J, Chippaux M, Barras F. Cellulase egz of Erwinia chrysanthemi:
662 Structural organization and importance of his98 and glu133 residues for catalysis. Protein Eng
663 Des Sel 1991;4:325–333. doi: 10.1093/protein/4.3.325
664 90. Palumbo JD, Sullivan RF, Kobayashi DY. Molecular characterization and expression in
665 Escherichia coli of three β-1,3-glucanase genes from Lysobacter enzymogenes strain N4-7. J
666 Bacteriol 2003;185:4362–4370. doi: 10.1128/JB.185.15.4362-4370.2003

667 91. Sugimoto K, Senda T, Aoshima H, Masai E, Fukuda M, et al. Crystal structure of an aromatic
668 ring opening dioxygenase LigAB, a protocatechuate 4,5-dioxygenase, under aerobic conditions.
669 Structure 1999;7:953–965. doi: 10.1016/S0969-2126(99)80122-1
670 92. Stehr M, Diekmann H, Smau L, Seth O, Ghisla S, et al. A hydrophobic sequence motif
671 common to N-hydroxylating enzymes. Trends Biochem Sci 1998;23:56–57. doi: 10.1016/S0968-
672 0004(97)01166-3
673 93. Kauppi B, Lee K, Carredano E, Parales RE, Gibson DT, et al. Structure of an aromatic-ring-
674 hydroxylating dioxygenasenaphthalene 1,2-dioxygenase. Structure 1998;6:571–586. doi: 10.1016/
675 S0969-2126(98)00059-8
676 94. Tsuchiya T, Ohta H, Okawa K, Iwamatsu A, Shimada H, et al. Cloning of chlorophyllase, the
677 key enzyme in chlorophyll degradation: Finding of a lipase motif and the induction by methyl
678 jasmonate. Proc Natl Acad Sci U S A 1999;96:15362–15367. doi: 10.1073/pnas.96.26.15362
679 95. Park SY, Chao X, Gonzalez-Bonet G, Beel BD, Bilwes AM, et al. Structure and function of an
680 unusual family of protein phosphatases: The bacterial chemotaxis proteins CheC and CheX. Mol
681 Cell 2004;16:563–574. doi: 10.1016/j.molcel.2004.10.018
682 96. Holmgren A, Bränden CL. Crystal structure of chaperone protein PapD reveals an
683 immunoglobulin fold. Nature 1989;342:248–251. doi: 10.1038/342248a0
684 97. Draper J, Karplus K, Ottemann KM. Identification of a chemoreceptor zinc-binding domain
685 common to cytoplasmic bacterial chemoreceptors. J Bacteriol 2011;193:4338–4345. doi: 10.1128/
686 JB.05140-11
687 98. Szurmant H, Ordal GW. Diversity in Chemotaxis Mechanisms among the Bacteria and
688 Archaea. Microbiol Mol Biol Rev 2004;68:301–319. doi: 10.1128/mmbr.68.2.301-319.2004
689 99. Ide N, Kutsukake K. Identification of a novel Escherichia coli gene whose expression is
690 dependent on the flagellum-specific sigma factor, FliA, but dispensable for motility development.
691 Gene 1997;199:19–23. doi: 10.1016/S0378-1119(97)00233-3
692 100. Pelicic V. Type IV pili: e pluribus unum? Mol Microbiol 2008;68:827–837. doi: 10.1111/j.1365-
693 2958.2008.06197.x

694 101. Serizawa M, Yamamoto H, Yamaguchi H, Fujita Y, Kobayashi K, et al. Systematic analysis of
695 SigD-regulated genes in Bacillus subtilis by DNA microarray and Northern blotting analyses. Gene
696 2004;329:125–136. doi: 10.1016/j.gene.2003.12.024
697 102. Martinez RM, Dharmasena MN, Kirn TJ, Taylor RK. Characterization of two outer membrane
698 proteins, FlgO and FlgP, that influence Vibrio cholerae motility. J Bacteriol 2009;191:5669–5679.
699 doi: 10.1128/JB.00632-09
700 103. Bäckman M, Källström H, Jonsson AB. The phase-variable pilus-associated protein PilC is
701 commonly expressed in clinical isolates of Neisseria gonorrhoeae, and shows sequence variability
702 among strains. Microbiology 1998;144:149–156. doi: 10.1099/00221287-144-1-149
703 104. Kawamoto T, Noshiro M, Shen M, Nakamasu K, Hashimoto K, et al. Structural and
704 phylogenetic analyses of RGD-CAP/βig-h3, a fasciclin- like adhesion protein expressed in chick
705 chondrocytes. Biochim Biophys Acta - Gene Struct Expr 1998;1395:288–292. doi: 10.1016/S0167-
706 4781(97)00172-3
707 105. Alm RA, Hallinan JP, Watson AA, Mattick JS. Fimbrial biogenesis genes of Pseudomonas
708 aeruginosa: pilW and pilX increase the similarity of type 4 fimbriae to the GSP protein-secretion
709 systems and pilY1 encodes a gonococcal PilC homologue. Mol Microbiol 1996;22:161–173. doi:
710 10.1111/j.1365-2958.1996.tb02665.x
711 106. Nambu T, Kutsukake K. The Salmonella FlgA protein, a putative periplasmic chaperone
712 essential for flagellar P ring formation. Microbiology 2000;146:1171–1178. doi: 10.1099/00221287-
713 146-5-1171
714 107. Funa N, Ohnishi Y, Ebizuka Y, Horinouchi S. Alteration of reaction and substrate specificity of
715 a bacterial type III polyketide synthase by site-directed mutagenesis. Biochem J 2002;367:781–
716 789. doi: 10.1042/BJ20020953
717 108. Ross P, Mayer R, Benziman M. Cellulose biosynthesis and function in bacteria. Microbiol
718 Rev;55. Epub ahead of print 1991. doi: 10.1128/mmbr.55.1.35-58.1991.
719 109. Matthysse AG. Role of bacterial cellulose fibrils in Agrobacterium tumefaciens infection. J
720 Bacteriol 1983;154:906–915. doi: 10.1128/jb.154.2.906-915.1983

721 110. Jones DL. Organic acids in the rhizosphere - A critical review. Plant Soil 1998;205:25–44.
722 doi: 10.1023/A:1004356007312
723 111. de Souza RSC, Armanhi JSL, Damasceno N de B, Imperial J, Arruda P. Genome Sequences
724 of a Plant Beneficial Synthetic Bacterial Community Reveal Genetic Features for Successful Plant
725 Colonization. Front Microbiol 2019;10:1779. doi: 10.3389/fmicb.2019.01779
726 112. Desbrosses GG, Kopka J, Udvardi MK. Lotus japonicus metabolic profiling. Development of
727 gas chromatography-mass spectrometry resources for the study of plant-microbe interactions. In:
728 Plant Physiology. American Society of Plant Biologists; 2005. pp. 1302–1318. doi:
729 10.1104/pp.104.054957
730 113. Liu CF, Tonini L, Malaga W, Beau M, Stella A, et al. Bacterial protein-O-mannosylating
731 enzyme is crucial for virulence of Mycobacterium tuberculosis. Proc Natl Acad Sci U S A
732 2013;110:6560–6565. doi: 10.1073/pnas.1219704110
733 114. Fernández-Álvarez A, Elias-Villalobos A, Ibeas JI. The O-mannosyltransferase PMT4 is
734 essential for normal appressorium formation and penetration in Ustilago maydis. Plant Cell
735 2009;21:3397–3412. doi: 10.1105/tpc.109.065839
736 115. Planamente S, Mondy S, Hommais F, Vigouroux A, Moréra S, et al. Structural basis for
737 selective GABA binding in bacterial pathogens. Mol Microbiol 2012;86:1085–1099. doi:
738 10.1111/mmi.12043
739 116. Li M, Guo R, Yu F, Chen X, Zhao H, et al. Indole-3-acetic acid biosynthesis pathways in the
740 plant-beneficial bacterium arthrobacter pascens zz21. Int J Mol Sci 2018;19:443. doi:
741 10.3390/ijms19020443
742 117. Chevrot R, Rosen R, Haudecoeur E, Cirou A, Shelp BJ, et al. GABA controls the level of
743 quorum-sensing signal in Agrobacterium tumefaciens. Proc Natl Acad Sci U S A 2006;103:7460–
744 7464. 10.1073/pnas.0600313103
745 118. Park DH, Mirabella R, Bronstein PA, Preston GM, Haring MA, et al. Mutations in γ-
746 aminobutyric acid (GABA) transaminase genes in plants or Pseudomonas syringae reduce
747 bacterial virulence. Plant J 2010;64:318–330. doi: 10.1111/j.1365-313X.2010.04327.x

748 119. Vernikos G, Medini D, Riley DR, Tettelin H. Ten years of pan-genome analyses. Current
749 Opinion in Microbiology 2015;23:148–154. doi: 10.1016/j.mib.2014.11.016
750 120. Tettelin H, Riley D, Cattuto C, Medini D. Comparative genomics: the bacterial pan-genome.
751 Current Opinion in Microbiology 2008;11:472–477. doi: 10.1016/j.gde.2005.09.006
752 121. Moran NA. Microbial minimalism: Genome reduction in bacterial pathogens. Cell
753 2002;108:583–586. doi: 10.1016/S0092-8674(02)00665-7
754 122. Wixon J. Reductive evolution in bacteria: Buchnera sp., Rickettsia prowazekii and
755 Mycobacterium leprae. 2001. Epub ahead of print 2001. doi: 10.1002/cfg.70.
756 123. Merhej V, Royer-Carenzi M, Pontarotti P, Raoult D. Massive comparative genomic analysis
757 reveals convergent evolution of specialized bacteria. Biol Direct 2009;4:13. doi: 10.1186/1745-
758 6150-4-13
759 124. Andersson SGE, Zomorodipour A, Andersson JO, Sicheritz-Ponte T, Cecilia U, et al. The
760 genome sequence of Rickettsia prowazekii and the origin of mitochondria. 1998;396. doi:
761 10.1038/2409
762 125. Georgiades K, Raoult D. Defining pathogenic bacterial species in the genomic era. Front
763 Microbiol 2011;1:151. doi: 10.3389/fmicb.2010.00151
764 126. Assis RDAB, Polloni LC, Patané JSL, Thakur S, Felestrino ÉB, et al. Identification and
765 analysis of seven effector protein families with different adaptive and evolutionary histories in
766 plant-associated members of the Xanthomonadaceae. Sci Rep;7. Epub ahead of print 1
767 December 2017. doi: 10.1038/s41598-017-16325-1.
768 127. Bernal P, Llamas MA, Filloux A. Type VI secretion systems in plant-associated bacteria.
769 Environ Microbiol 2018;20:1–15. doi: 10.1111/1462-2920.13956
770 128. Pallen MJ, Wren BW. Bacterial pathogenomics. Nature 2007;449:835–842. doi:
771 10.1038/nature06248
772 129. Weissman KJ, Leadlay PF. Combinatorial biosynthesis of reduced polyketides. Nature
773 Reviews Microbiology 2005;3:925–936. doi: 10.1038/nrmicro1287

774 130. Grünewald J, Marahiel MA. Chemoenzymatic and Template-Directed Synthesis of Bioactive
775 Macrocyclic Peptides. Microbiol Mol Biol Rev 2006;70:121–146. doi: 10.1128/mmbr.70.1.121-
776 146.2006
777 131. Khalid S, Baccile JA, Spraker JE, Tannous J, Imran M, et al. NRPS-Derived Isoquinolines
778 and Lipopetides Mediate Antagonism between Plant Pathogenic Fungi and Bacteria. ACS Chem
779 Biol 2018;13:171–179. doi: 10.1021/acschembio.7b00731
780 132. Dias R, Torkamani A. Artificial intelligence in clinical and genomic diagnostics. Genome
781 Medicine 2019;11:70. doi: 10.1186/s13073-019-0689-8
782 133. Iversen KH, Rasmussen LH, Al-Nakeeb K, Armenteros JJA, Jensen CS, et al. Similar
783 genomic patterns of clinical infective endocarditis and oral isolates of Streptococcus sanguinis and
784 Streptococcus gordonii. Sci Rep 2020;10:1–11. doi: 10.1038/s41598-020-59549-4
785 134. Qu K, Guo F, Liu X, Lin Y, Zou Q. Application of machine learning in microbiology. Front
786 Microbiol 2019;10:827. doi: 10.3389/fmicb.2019.00827
787 135. Tarca AL, Carey VJ, Chen X wen, Romero R, Drăghici S. Machine learning and its
788 applications to biology. PLoS Comput Biol 2007;3:e116. doi: 10.1371/journal.pcbi.0030116

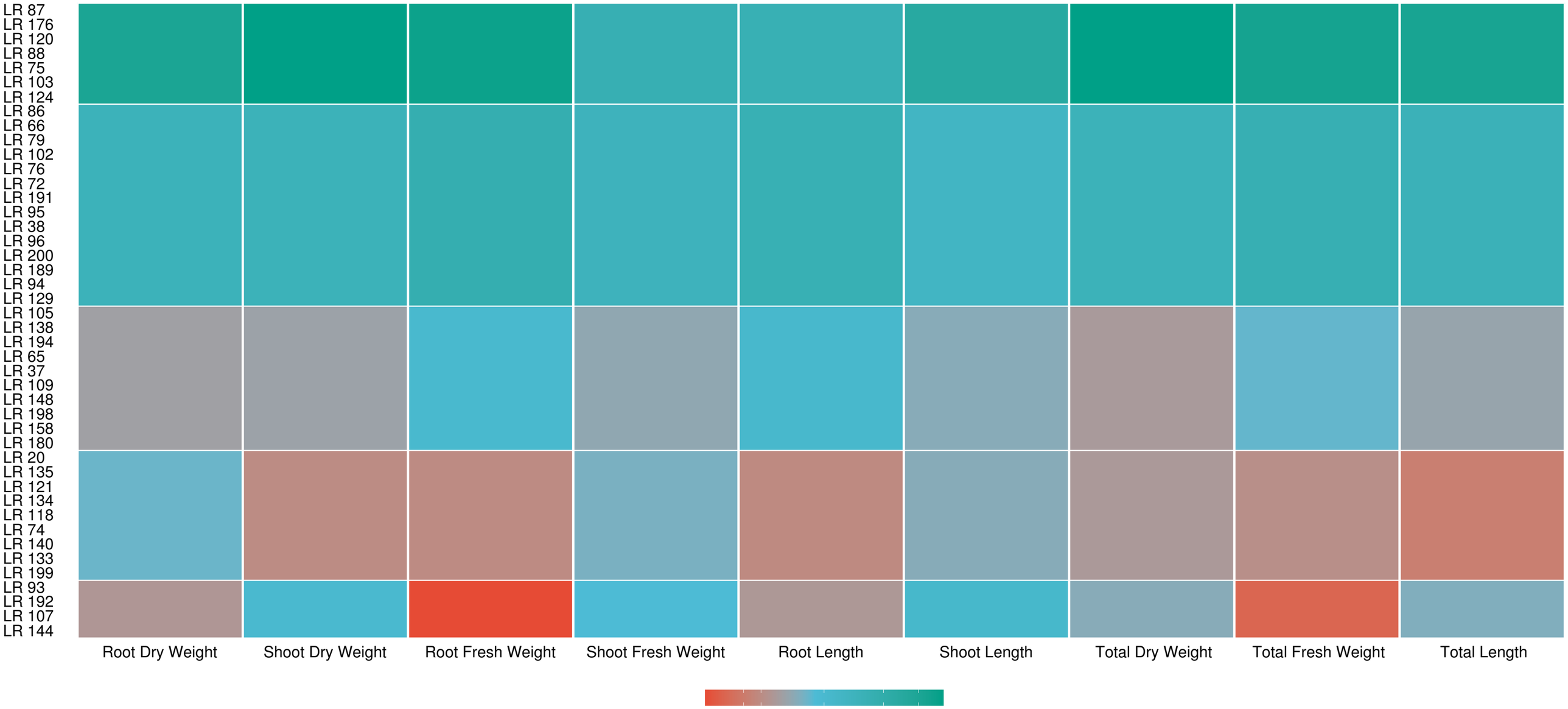
LR 87
LR 176
LR 120
LR 88
LR 75
LR 103
LR 124
LR 86
LR 66
LR 79
LR 102
LR 76
LR 72
LR 191
LR 95
LR 38
LR 96
LR 200
LR 189
LR 94
LR 129
LR 105
LR 138
LR 194
LR 65
LR 37
LR 109
LR 148
LR 198
LR 158
LR 180
LR 20
LR 135
LR 121
LR 134
LR 118
LR 74
LR 140
LR 133
LR 199
LR 93
LR 192
LR 107
LR 144
Root Dry Weight
Shoot Dry Weight
Root Fresh Weight
Shoot Fresh Weight
Root Length
Shoot Length
Total Dry Weight
Total Fresh Weight
Total Length

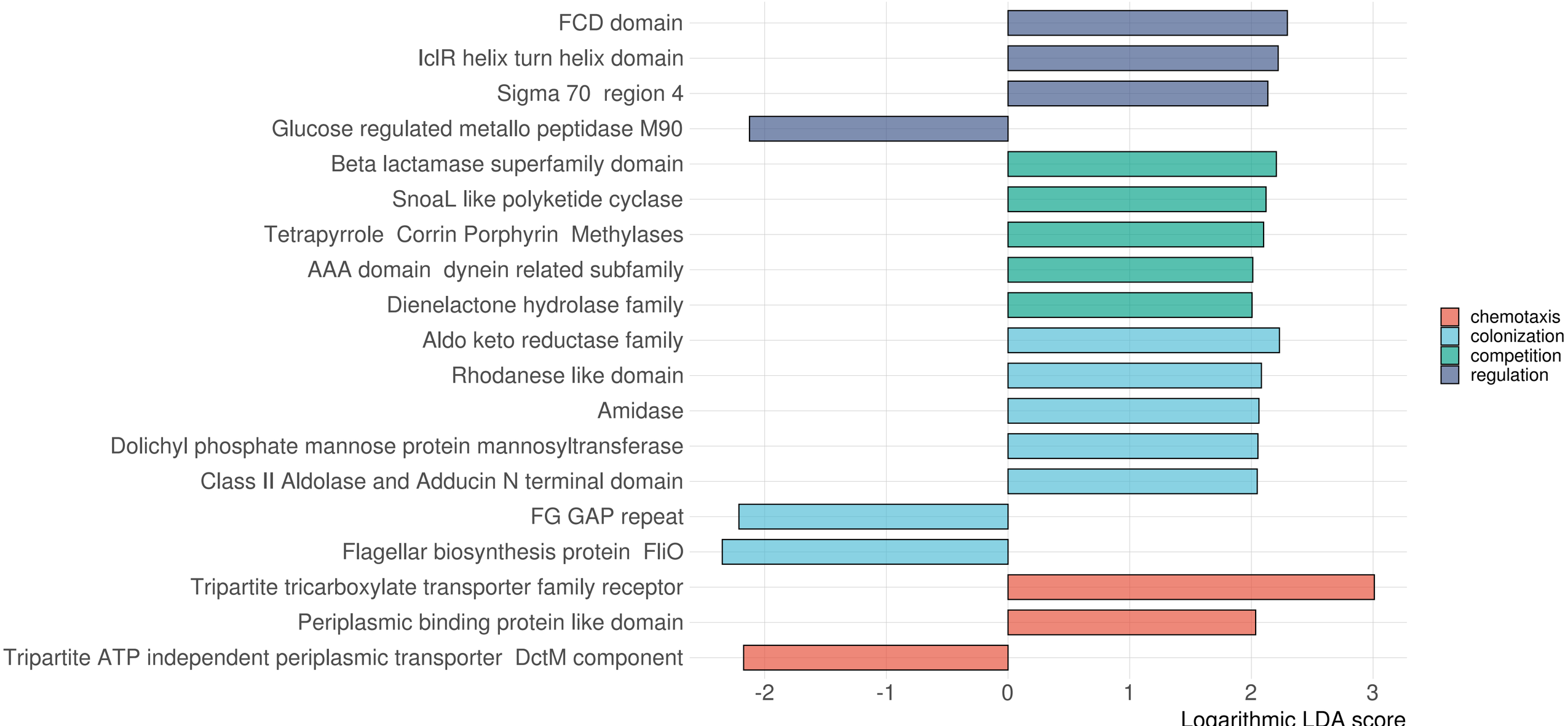
FCD domain
IclR helix turn helix domain
Sigma 70 region 4
Glucose regulated metallo peptidase M90
Beta lactamase superfamily domain
SnoaL like polyketide cyclase
Tetrapyrrole Corrin Porphyrin Methylases
AAA domain dynein related subfamily
Dienelactone hydrolase family
Aldo keto reductase family
Rhodanese like domain
Amidase
Dolichyl phosphate mannose protein mannosyltransferase
Class II Aldolase and Adducin N terminal domain
FG GAP repeat
Flagellar biosynthesis protein FliO
Tripartite tricarboxylate transporter family receptor
Periplasmic binding protein like domain
Tripartite ATP independent periplasmic transporter DctM component
-2
-1
0
1
2
3
Logarithmic LDA score
chemotaxis
colonization
competition
regulation

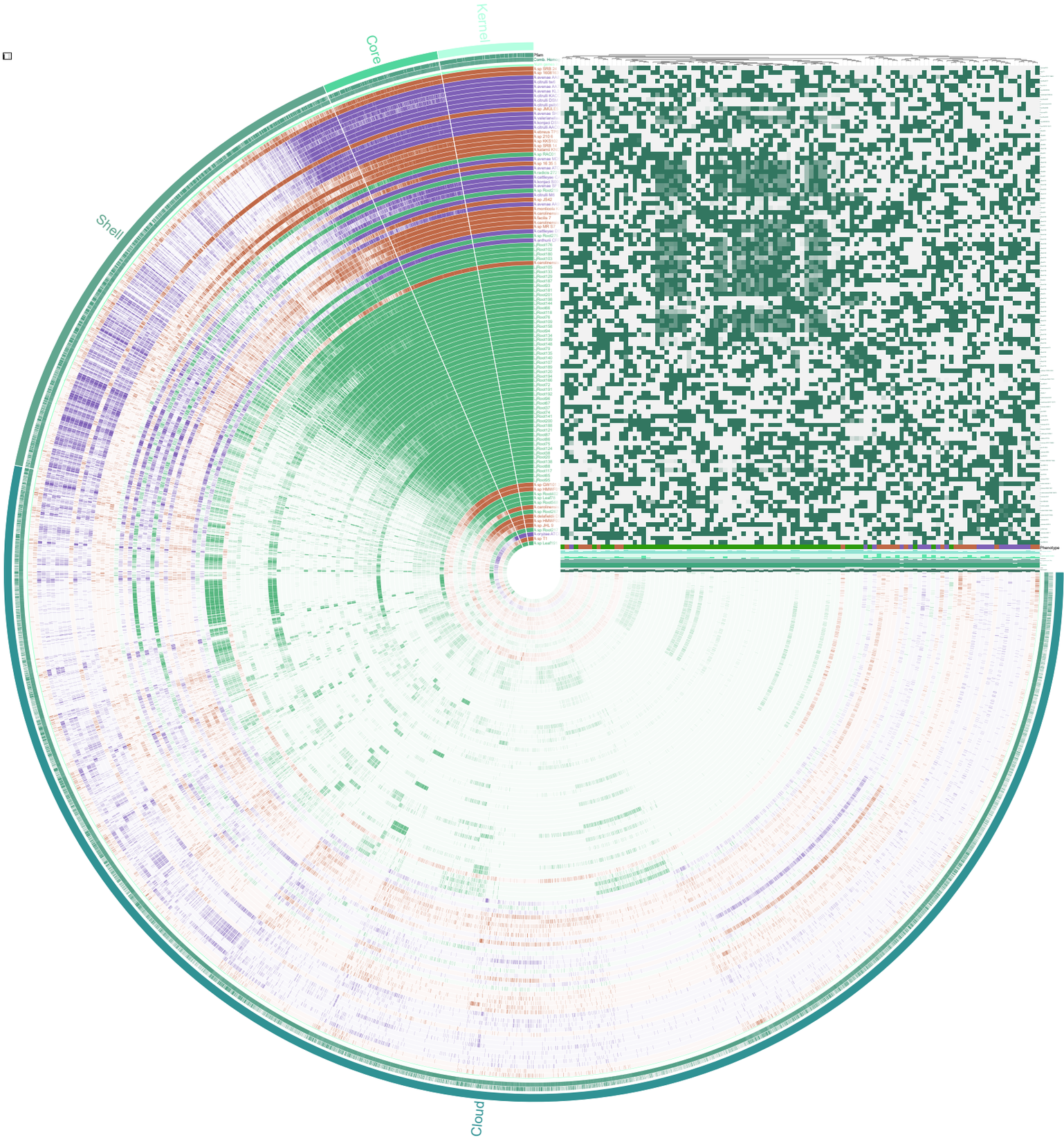

pathogen (21) free-living (23) commensal (62)

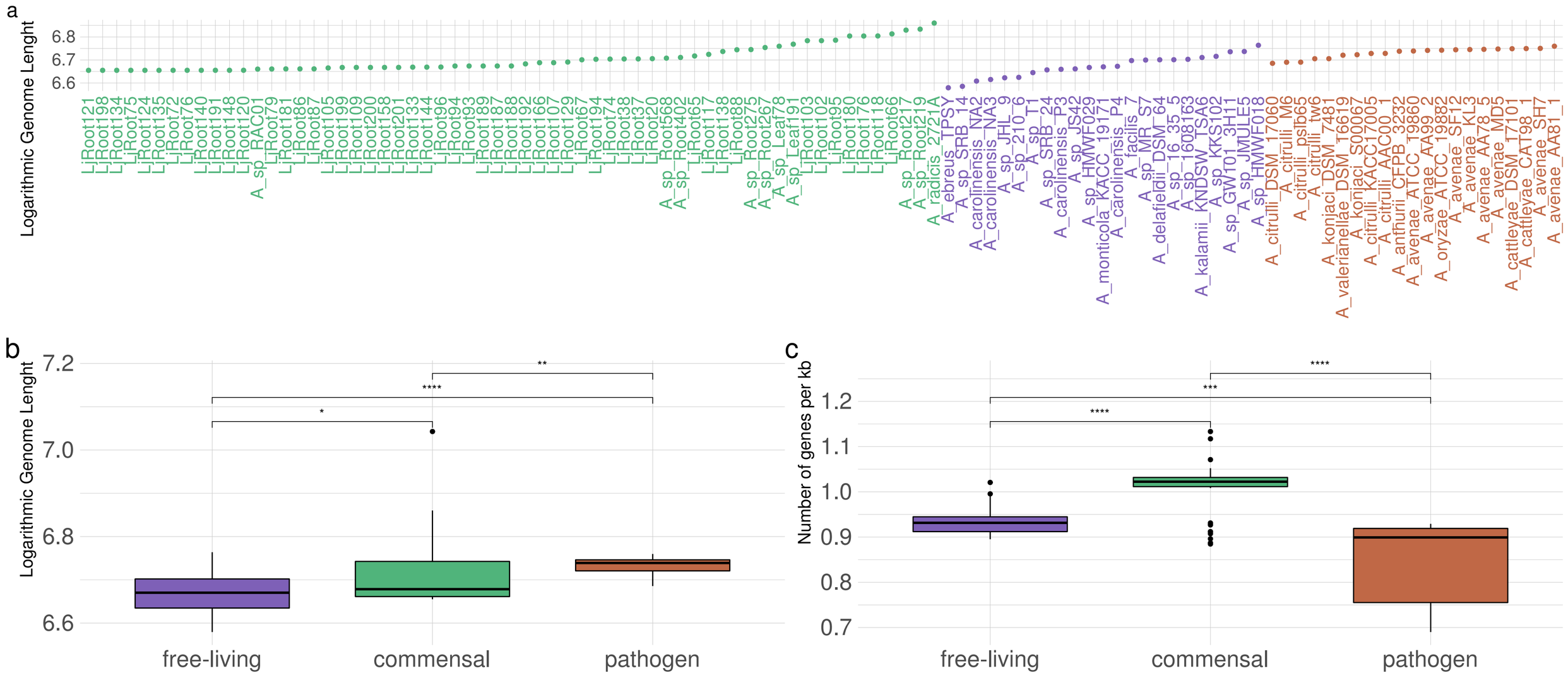
a
Logarithmic Genome Lenght
6.8
6.7
6.6
LiRoot121
LiRoot198
LiRoot134
LiRoot75
LiRoot124
LiRoot135
LiRoot72
LiRoot76
LiRoot140
LiRoot191
LiRoot148
LiRoot120
A_sp_RAC01
LiRoot79
LiRoot181
LiRoot86
LiRoot87
LiRoot105
LiRoot199
LiRoot109
LiRoot200
LiRoot158
LiRoot201
LiRoot133
LiRoot144
LiRoot96
LiRoot94
LiRoot93
LiRoot189
LiRoot187
LiRoot188
LiRoot192
LiRoot166
LiRoot107
LiRoot129
LiRoot67
LiRoot194
LiRoot74
LiRoot38
LiRoot37
LiRoot20
A_sp_Root568
A_sp_Root402
LiRoot65
LiRoot117
LiRoot138
LiRoot88
A_sp_Root275
A_sp_Root267
A_sp_Leaf78
A_sp_Leaf191
LiRoot103
LiRoot102
LiRoot95
LiRoot180
LiRoot176
LiRoot118
LiRoot66
A_sp_Root217
A_sp_Root219
A_radicis_2721A
A_ebreus_TPSY
A_sp_SRB_14
A_carolinensis_NA2
A_carolinensis_NA3
A_sp_JHL_9
A_sp_210_6
A_sp_T1
A_sp_SRB_24
A_carolinensis_P3
A_sp_JS42
A_sp_HMWF029
A_monticola_KACC_19171
A_carolinensis_P4
A_facilis_7
A_sp_MR_S7
A_delafieldii_DSM_64
A_sp_16_35_5
A_sp_1608163
A_kalamii_KNDSW_TSA6
A_sp_KKS102
A_sp_GW101_3H11
A_sp_JMULE5
A_sp_HMWF018
A_citrulli_DSM_17060
A_citrulli_M6
A_citrulli_psl65
A_citrulli_tw6
A_konjaci_DSM_7481
A_konjaci_T6619
A_valerianellae_DSM_
A_konjaci_S00067
A_citrulli_KACC17005
A_citrulli_AAC00_1
A_anthurii_CFPB_3232
A_avenae_ATCC_19860
A_avenae_AA99_2
A_oryzae_ATCC_19882
A_avenae_SF12
A_avenae_KL3
A_avenae_AA78_5
A_avenae_MD5
A_cattleyae_DSM_17101
A_cattleyae_CAT98_1
A_avenae_SH7
A_avenae_AA81_1
b
Logarithmic Genome Lenght
7.2
7.0
6.8
6.6
**
****
*
free-living
commensal
pathogen
c
Number of genes per kb
1.2
1.1
1.0
0.9
0.8
0.7
****
***
****
free-living
commensal
pathogen

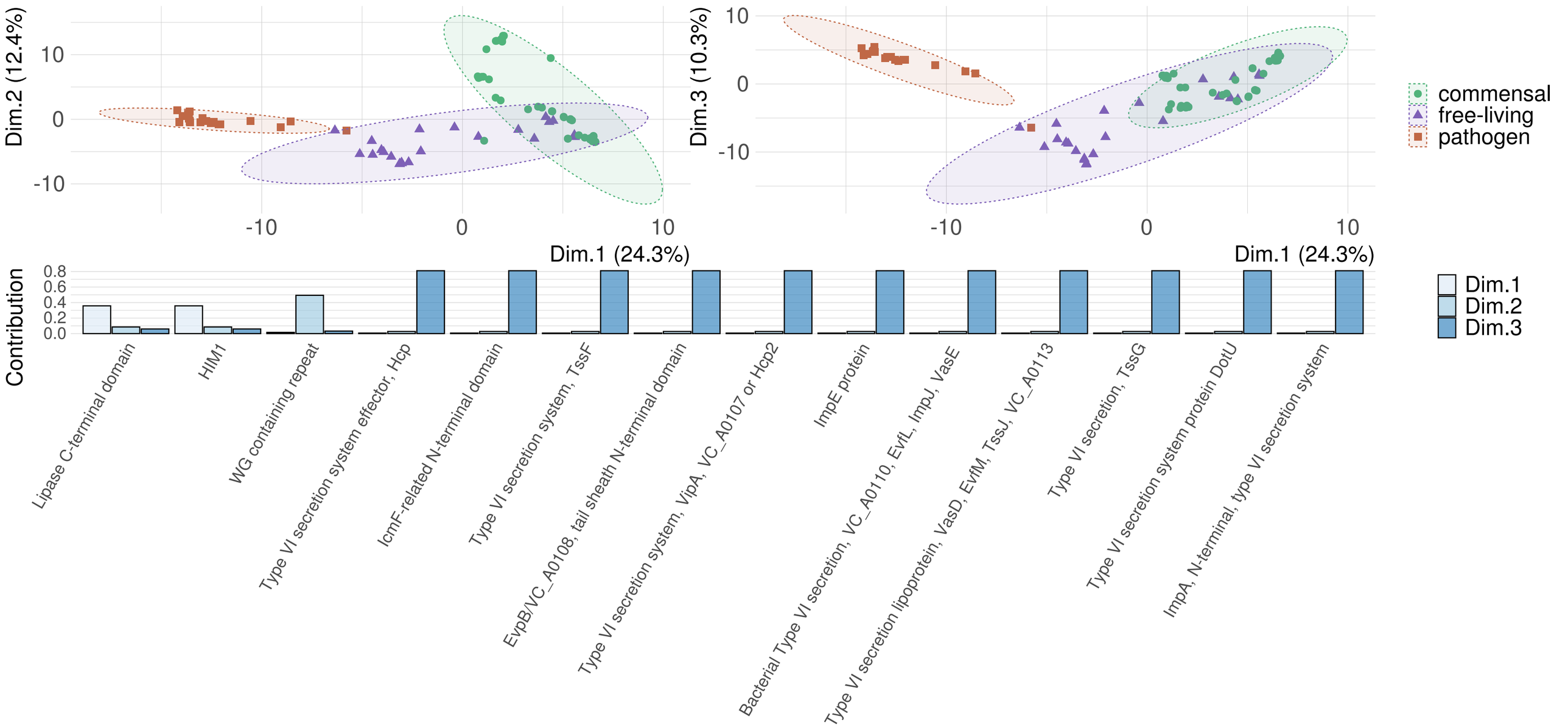
Dim.2 (12.4%)
Dim.1 (24.3%)
Dim.3 (10.3%)
Dim.1 (24.3%)
commensal
free-living
pathogen
Contribution
Dim.1
Dim.2
Dim.3
Lipase C-terminal domain
HIM1
WG containing repeat
Type VI secretion system effector, Hcp
IcmF-related N-terminal domain
Type VI secretion system, TssF
EvpB/VC_A0108, tail sheath N-terminal domain
Type VI secretion system, VipA, VC_A0107 or Hcp2
ImpE protein
Bacterial Type VI secretion, VC_A0110, EvfL, ImpJ, VasE
Type VI secretion lipoprotein, VasD, EvfM, TssJ, VC_A0113
Type VI secretion, TssG
Type VI secretion system protein DotU
ImpA, N-terminal, type VI secretion system

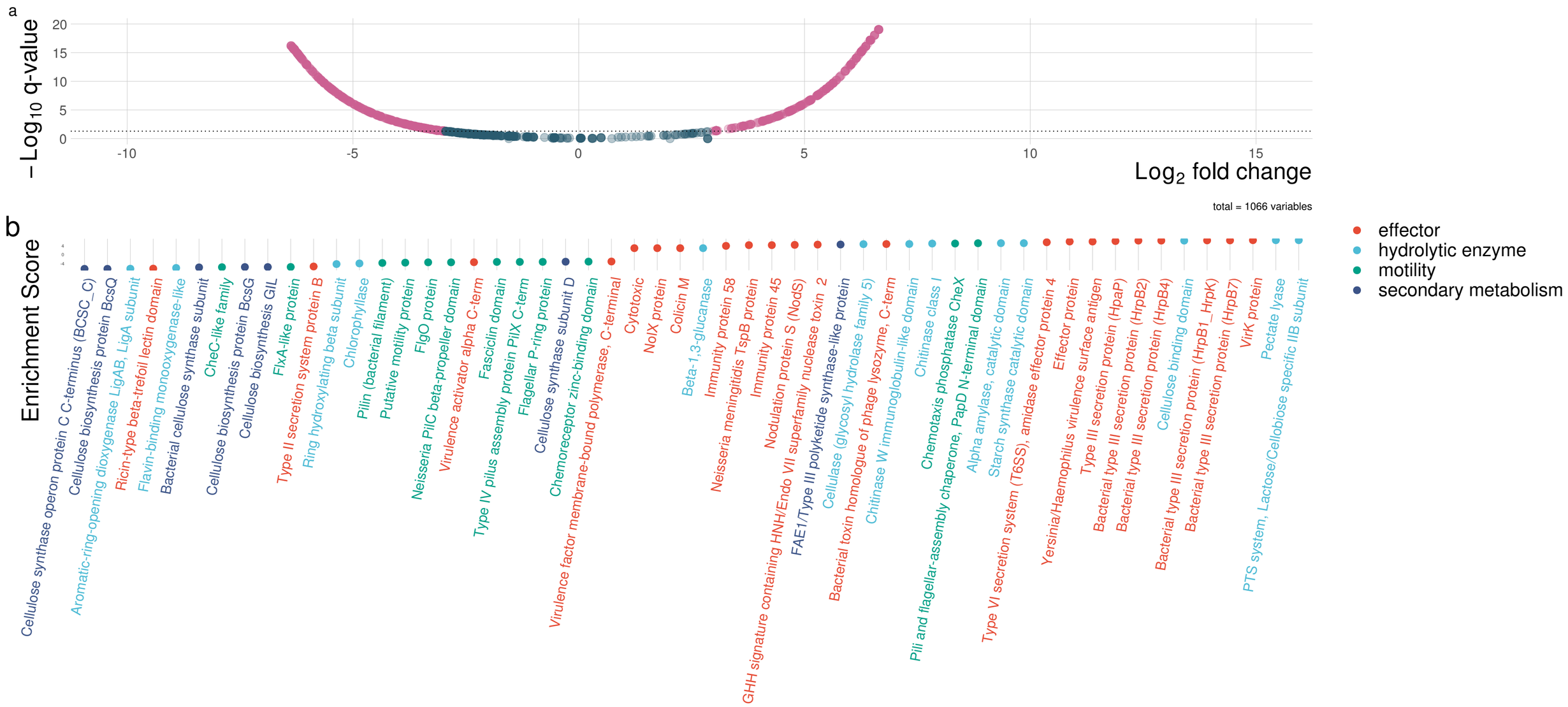
a
– Log10 q-value
20
15
10
5
0
-10
-5
0
5
10
15
Log2 fold change
total = 1066 variables
b
Enrichment Score
Cellulose synthase operon protein C C-terminus (BCSC_C)
Cellulose biosynthesis protein BcsQ
Aromatic-ring-opening dioxygenase LigAB, LigA subunit
Ricin-type beta-trefoil lectin domain
Flavin-binding monooxygenase-like
Bacterial cellulose synthase subunit
CheC-like family
Cellulose biosynthesis protein BcsG
Cellulose biosynthesis GIL
FlxA-like protein
Type II secretion system protein B
Ring hydroxylating beta subunit
Chlorophyllase
Pilin (bacterial filament)
Putative motility protein
FlgO protein
Neisseria PilC beta-propeller domain
Virulence activator alpha C-term
Fasciclin domain
Type IV pilus assembly protein PilX C-term
Flagellar P-ring protein
Cellulose synthase subunit D
Chemoreceptor zinc-binding domain
Virulence factor membrane-bound polymerase, C-terminal
Cytotoxic
NolX protein
Colicin M
Beta-1,3-glucanase
Immunity protein 58
Neisseria meningitidis TspB protein
Immunity protein 45
Nodulation protein S (NodS)
GHH signature containing HNH/Endo VII superfamily nuclease toxin 2
FAE1/Type III polyketide synthase-like protein
Cellulase (glycosyl hydrolase family 5)
Bacterial toxin homologue of phage lysozyme, C-term
Chitinase W immunoglobulin-like domain
Chitinase class I
Chemotaxis phosphatase CheX
Pili and flagellar-assembly chaperone, PapD N-terminal domain
Alpha amylase, catalytic domain
Starch synthase catalytic domain
Type VI secretion system (T6SS), amidase effector protein 4
Effector protein
Yersinia/Haemophilus virulence surface antigen
Type III secretion protein (HpaP)
Bacterial type III secretion protein (HrpB2)
Bacterial type III secretion protein (HrpB4)
Cellulose binding domain
Bacterial type III secretion protein (HrpB1_HrpK)
Bacterial type III secretion protein (HrpB7)
VirK protein
Pectate lyase
PTS system, Lactose/Cellobiose specific IIB subunit
effector
hydrolytic enzyme
motility
secondary metabolism

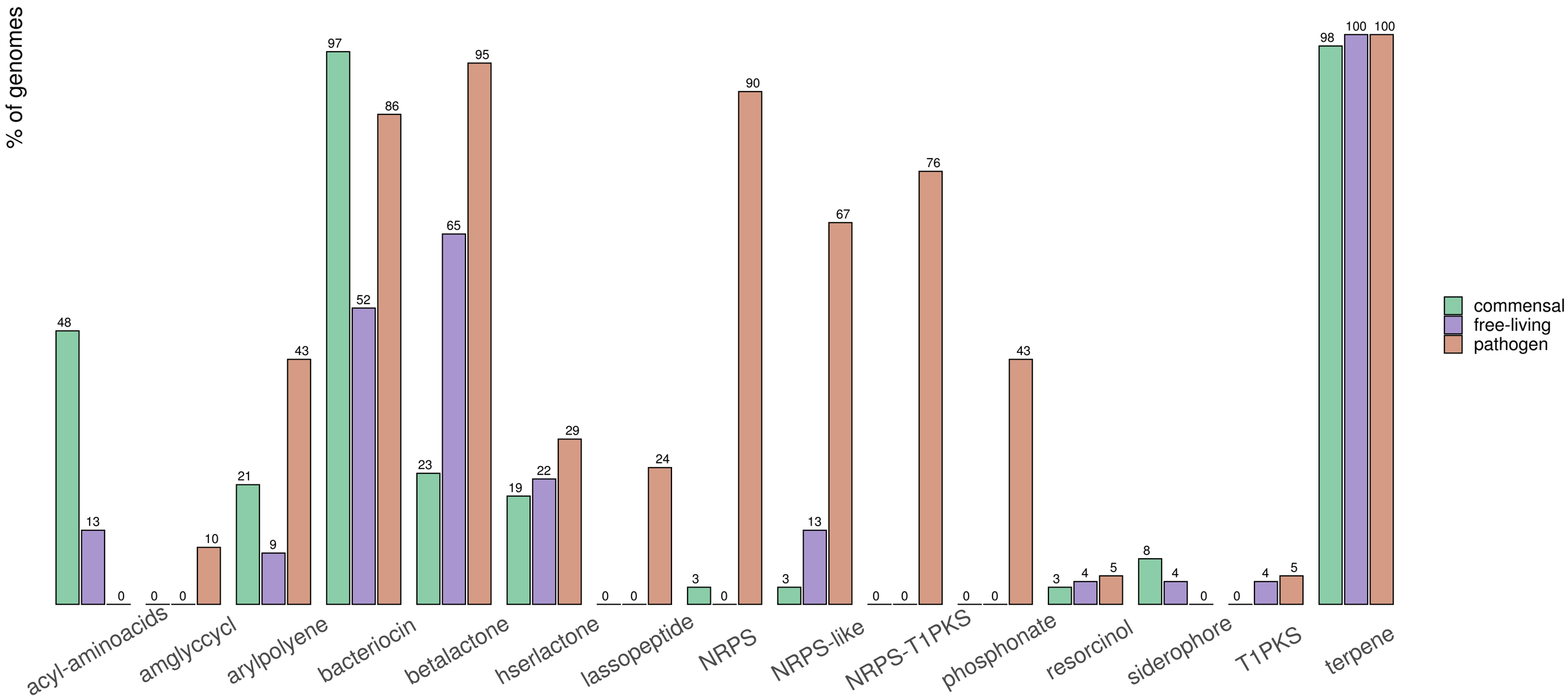
% of genomes
48
13
0
0
0
10
21
9
43
97
52
86
23
65
95
19
22
29
0
0
24
3
0
90
3
13
67
0
0
76
0
0
43
3
4
5
8
4
0
0
4
5
98
100
100
acyl-aminoacids
amglyccycl
arylpolyene
bacteriocin
betalactone
hserlactone
lassopeptide
NRPS
NRPS-like
NRPS-T1PKS
phosphonate
resorcinol
siderophore
T1PKS
terpene
commensal
free-living
pathogen

FIGURES:

Fig.1: Heat-map showing the effects of single-strains on *Lotus japonicus* growth parameters as observed in the *L. japonicus* growth bioassays. Measures are shown as the median, for each observed group, of the percentage change from the control.

Fig.2: Bar-plot of the logarithmic scores from the Linear Discriminant analysis for the discriminant Pfams. Pfams are assigned to 4, color-coded, functional groups.

Fig.3: Anvi'o 6.2 circular representation of *Acidovorax* pan-genome and heat-map of average nucleotide identity across the genomes.

Fig.4: a) Dot-chart of individuals logarithmic genome length. b) box-plot of groups logarithmic genome length. c) box-plot of groups gene density expressed as number of genes per 1000 base-pairs. Significance was assessed by Student's t-test with Holm's correction ($p < 0.05$).

Fig.5: a) Ordination plot for the first and second component of the principal component analysis (PCA) b) Ordination for the first and third component of the PCA. c) Bar-plot of the Pfams with the highest contribution for first, second and third component of the PCA.

Fig.6: a) Volcano plot displaying Pfams enriched in commensal (left) and pathogenic strains (right). On the x axis is represented logarithmic fold change and on the y axis adjusted *q*-value. Dots are represented in red when crossing the significance threshold of 0.05. b) Dot-plot of the curated list of enriched Pfams related to host-microbe or microbe-microbe interaction. Each dot is color coded based on the functional family of assignment.

Fig.7: Bar-plot of the percentage of genomes per group featuring each of the retrieved biosynthesis gene clusters.